Effects of N doping on the electronic properties of a small carbon atomic chain with distinct sp^2 terminations: A first-principles study

Renato B. dos Santos,[1,*] R. Rivelino,[1,†] F. de Brito Mota,[1] and G. K. Gueorguiev[2,‡]

[1]*Instituto de Física, Universidade Federal da Bahia, 40210-340 Salvador, Bahia, Brazil*
[2]*Department of Physics, Chemistry and Biology, IFM, Linköping University, SE-58183 Linköping, Sweden*

Carbon nanostructures consisting of corannulene/coronene-like pieces connected by atomic chains and doped with nitrogen atoms have been addressed by carrying out first-principles calculations within the framework of the spin-polarized density functional theory. Our results show that the conformation, charge distributions, and spin states are significantly influenced by the nitrogen incorporation in comparison to these characteristics of similar pure carbon structures. Higher concentration of incorporated nitrogen leads to a smaller highest occupied molecular orbital–lowest unoccupied molecular orbital (HOMO-LUMO) gap and different conductive states near the Fermi level. In turn the different location of the N-incorporation sites allows switching on and off of the π-electron magnetism in these systems. We found that the rotational deformation of the terminations with respect to the carbon chain depends on the number and the location of the incorporated N atoms. The most stable N-doped structures exhibit a relative rotation of the terminations of approximately 90 degrees. These findings indicate that by controllable N doping one can tune the conducting channel of carbon chains connected to sp^2 terminations; thus obtaining low band-gap nano-units.

PACS number(s): 73.20.At, 73.20.Hb, 71.15.Nc

I. INTRODUCTION

The substitution of carbon by nitrogen in carbon-based nano-structured materials is perceived as a possibility of tuning their electronic and mechanical properties[1–3] for future applications in electronic and photonic devices. Nitrogen is an appropriate dopant for carbon-based systems, since it has a similar atomic radius as carbon and possesses 1 additional valence electron. Hence, this *n*-type doping can also lead to significant changes in the band gap of the corresponding carbon-based materials. For example, in graphene the nitrogen-doped carbon system can increase the durability and activity of a Pt catalyst,[4,5] while in fullerenelike thin solid films the N-doped system has been found to lead to high hardness combined with a high elasticity attributable to the cross-linking between curved basal planes.[6]

The substitution of C by N in a corannulene molecule or in a pentaindenocorannulene molecule gives an increment of the absorption energy of the carbon structures. Such increment is, however, strongly dependent on the incorporation site of the nitrogen atom.[7] In corannulene the stability of an N-doped system also depends on the nitrogen incorporation site.[8] Density-functional theory studies of N doping of graphenelike pieces have shown that N atoms can disrupt the delocalized double bond typical for the graphene sheets, improving the Pt-catalyst binding energy.[9]

Additionally by employing first-principles calculations of the electronic properties of N-doped graphene nanoribbons (GNRs), it was found that the incorporated nitrogen atoms prefer to distribute near the nanoribbon edges, thus exhibiting an impurity state below or above the Fermi level for the N-doped GNR. Again, electronic structure details depend on the nitrogen incorporation site.[10]

In the present work we investigate the structural and electronic impact of N incorporation in a carbon-atomic chain connecting 2 distinct terminations with sp^2 hybridizations. In principle these types of atomic chains could be experimentally fabricated from N-doped GNR by using a controlled electron-beam irradiation.[11] Our model system consists here in a corannulene–C_4–coronene structure (where –C_4– represents a one-dimensional atomic chain containing four carbon atoms). We consider between 1 and 3 nitrogen atoms occupying different carbon sites in this reference structure. In a previous work[12] we addressed the "pure carbon" coronene–C_n–coronene structure ($n = 3$–6), and we found that its electronic properties depend on its parity. Structures with an even number of C atoms in the chain are singlet (the total spin is 0) and those with an odd number of C atoms in the chain are triplet[12,13] (the total spin is 1).

The substitution of C by N in a structure like that is also expected to significantly change its magnetic properties,[14] thus providing templates with controllable magnetic properties and possible optoelectronic applications.[15–19] The model system containing a four carbon atom chain studied in this work has been chosen because such variants of the considered systems, with an even number of carbon atoms in the chain, possess the advantage of exhibiting larger band gaps, in comparison with similar systems containing an odd number of atoms in the chain.[12] To explore a higher structural diversity of nitrogen incorporation sites we have employed 1 coronene molecule and 1 corannulene molecule at the extremities of the chain, instead of symmetric systems consisting of 2 coronene molecules or 2 corannulene molecules.

II. METHODS AND CALCULATIONS

The calculations presented here were performed within density-functional theory (DFT) in the generalized gradient approximation (GGA),[20] using localized basis sets. All the model structures of the corannulene–C_4–coronene type and their N-doped products were optimized according to the procedures:

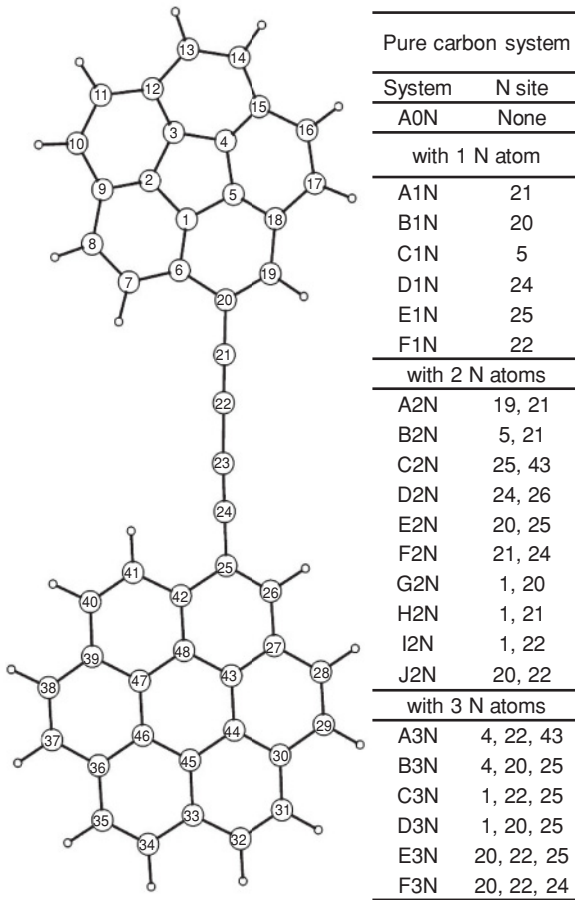(1) At the first stage we employed the Gaussian 03 code[21] to perform all-electron calculations within the hybrid

Pure carbon system	
System	N site
A0N	None
with 1 N atom	
A1N	21
B1N	20
C1N	5
D1N	24
E1N	25
F1N	22
with 2 N atoms	
A2N	19, 21
B2N	5, 21
C2N	25, 43
D2N	24, 26
E2N	20, 25
F2N	21, 24
G2N	1, 20
H2N	1, 21
I2N	1, 22
J2N	20, 22
with 3 N atoms	
A3N	4, 22, 43
B3N	4, 20, 25
C3N	1, 22, 25
D3N	1, 20, 25
E3N	20, 22, 25
F3N	20, 22, 24

FIG. 1. Identification map introducing the labeling for all model systems. Table at the right-hand side contains the system's labels (left column) and the sites of incorporation of the N atoms (right column).

GGA B3LYP exchange-correlation functional,[22,23] using the 6-31G(d,p) basis set. In the total 23 different structures were optimized; the first one being the pure carbon (corannulene–C$_4$–coronene) structure, and the remaining 22 structures resulting from substitution of selected C atom(s) by 1, 2, or 3 N atom(s) (see the nomenclature in Fig. 1). As we are dealing with large molecular systems, the Gaussian code is particularly a useful tool due especially to the fact that it provides very efficient analytic gradients for density-functional theory (DFT). This permits that the equilibrium geometry of all systems of interest are efficiently localized and additionally characterized as energy minimum structures using the harmonic frequency analysis.

(2) At the second stage all B3LYP/6-31G(d,p) optimized structures were used as input in the SIESTA program.[24] The advantage to switch to SIESTA for performing this task is attributable to its efficiency for treating the electronic structure of very large systems with good accuracy and also yielding a reliable interpretation of the spin-polarized electron density of states (DOS). In this case we employed the pure GGA scheme of Perdew, Burke, and Ernzerhof (PBE),[25] using norm-conserving pseudopotentials[26] as well as conjugate gradients algorithm for a second geometry-relaxation process. We

adopted a double ζ-pseudoatomic orbital basis set, which has been shown to be successful when addressing similar systems such as nanotubes,[27] nanochains,[28] and graphene.[28] After the reoptimization of all the 23 model systems, the DOS, charge density for the highest occupied molecular orbital (HOMO), and the lowest unoccupied molecular orbital (LUMO), as well as the spin densities were calculated.

To obtain the total DOS, first we carried out spin-polarized calculations using the Gaussian 03 code,[21] which locates a minimum structure for a fixed-spin multiplicity. The most stable structures found in this way were then submitted to the SIESTA's spin-polarized relaxation. In terms of the spin multiplicity, some of the obtained systems exhibit singlet states, while others appear in doublet or triplet states, depending on the number of dopant N atoms and their incorporation sites. The spin density is defined as the difference in the electron density of up and down electron spin densities.[29,30]

Additionally the cohesive energy (E_{coh}) of each model system was calculated. It is defined as the energy required for breaking the system into the isolated atomic species.[31] The cohesive energy per atom ($E_{coh/at}$) is given by

$$E_{coh/at} = -(E_{total} - n_c E_c - n_H E_H - n_N E_N)/M, \quad (1)$$

where E_{total}, E_C, E_H, and E_N are the total energies of an optimized system, an isolated carbon atom, an isolated hydrogen atom, and an isolated nitrogen atom, respectively. The coefficients n_C, n_H, and n_N represent the numbers of carbon, hydrogen, and nitrogen atoms, respectively. $M = n_C + n_N$ stays for the number of both carbon and nitrogen atoms.

III. RESULTS AND DISCUSSION

Figure 1 displays a scheme with the optimized undoped system. This prototypical system is quite useful as a reference (benchmark) to the structures doped with 1, 2, or 3 N atom(s). In the table provided at the right-hand side of the structure in Fig. 1 the positions of the nitrogen substitutions are listed in accordance to the pure carbon benchmark structure. Thus, each system is labeled by a symbol (left column of the table on Fig. 1). The structure bearing label A0N is the pure carbon prototype, while the structures labeled from A1N to F1N possess 1 N atom, A2N to J2N incorporate 2 N atoms, and A3N to F3N incorporate 3 N atoms. Our designation of each system (a string containing 2 letters and 1 number) uniquely identifies not only the number of N atoms incorporated but also the site(s) of the N substitutions.

In the following discussion we shall compare the electronic properties of the 22 N-doped optimized structures to the benchmark system (corannulene–C$_4$–coronene).

A. The benchmark system

As expected after geometry optimization the coronene part of the system conserves its planar shape, while the corannulene part maintains its usual curvature, in agreement with works by others.[32,33] The carbon chain preserves its linear geometry but the corannulene molecule undergoes a significant rotation of about 10 degrees in relation to the coronene plane. Except for this rotational deformation, the structural properties obtained here agree with our previous results performed within all-
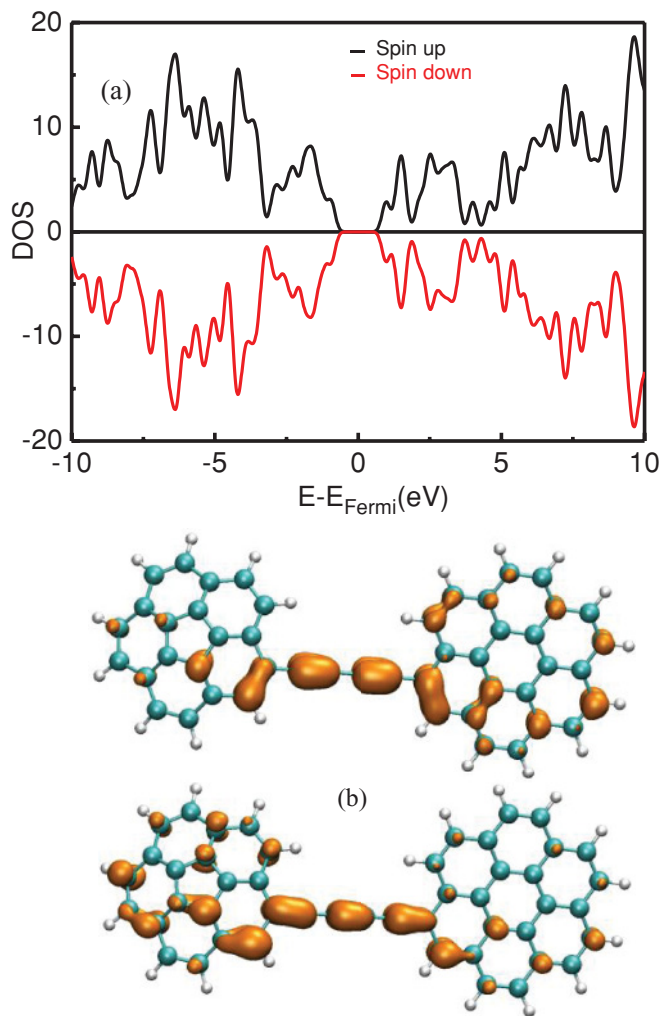
FIG. 2. (Color online) (a) Calculated spin-polarized DOS for the benchmark system A0N (a typical closed-shell system). (b) Iso-surface of the HOMO (top) and LUMO (bottom) spin densities for A0N.

electron DFT for the coronene–C_n–coronene structures ($n = 3$–6),[12] for which the 2 coronene molecules remain in the same plane.

The bond lengths obtained in the chain part of the system, starting the sequence from the corannulene part toward the coronene part, are as follows: 1.418, 1.238, 1.355, 1.238, and 1.420 Å. While in our previous work[12] for a symmetric coronene–C_4–coronene system the sequence reads 1.420, 1.238, 1.355, 1.238, and 1.420 Å. The effect of curvature in one of the terminations (induced by the replacement of coronene for corannulene) brings a negligible change in the bond length closest to this termination. As a consequence the electronic structure of the carbon chain in both these systems is rather similar.

In Fig. 2(a) the plotting of the spin-polarized DOS of the corannulene–C_4–coronene system is shown. As expected for this structure, the up and down DOS are symmetric; i.e., there is no liquid spin in the benchmark structure because both terminations form closed-shell systems. The calculated value of the HOMO-LUMO gap is 1.92 eV, which is very similar to that (1.97 eV) obtained for the coronene–C_4–coronene

sytem.[12] By examining the charge density of the frontier molecular orbitals, displayed in Fig. 2(b), the HOMO density is concentrated on the alternating C–C bonds, with less electron density at the bond between the chain and either the corannulene or the coronene terminations [Fig. 2(b), top]. This result is also in agreement with our previous analysis of the frontier molecular orbitals in related systems.[12] Thus, the presence of curvature (which can be seen as a kind of geometric defect in graphenelike networks) in one of the terminations does not introduce noticeable changes in the electronic distribution of the pure carbon chain.

B. Systems incorporating 1 N atom

For the total, after taking into account the symmetries, we obtain six different systems incorporating 1 N atom; i.e., A1N to F1N, which exhaust several structural possibilities, and we consider the most noteworthy of them in the present discussion.

Forthe system incorporating 1 N atom, the relaxed structures exhibit distinct structural and electronic differences when compared to the benchmark system [see Fig. 2(b)]. The bond lengths near the N atom in the most cases change significantly with respect to the reference structure. In B1N the bond length 20–21 (see Fig. 1 for reading the labels) is 1.34 Å, while the equivalent bond length in the benchmark system (A0N) is 1.42 Å. In F1N the bond length 19–20 is 1.45 Å, while the equivalent bond length in A0N is 1.42 Å; i.e., a small increment of 0.03 Å attributable to the N atom incorporated at site 22. For the same system, the bond length 20–21 (next to the N substitution) is about 0.05 Å shorter in comparison to the equivalent bond length in the pure carbon system. These values illustrate that the N incorporation in such low dimensional systems changes not only the bond length close to the N site but affects the system as a whole.

It is noteworthy that the systems incorporating 1 N atom undergo a large rotational deformation when the N atom is inserted in the chain. The angle of the relative rotation of the coronene with respect to the corannulene terminations increases to approximately 90 degrees. The inclusion of 1 N atom in the pure carbon structure breaks the π-electron symmetry along the chain. Moreover, when the N atom is incorporated in the chain, the terminations suffer a large rotational deformation. This finding indicates that the lone-pair orientation in N atoms plays an important role for the electron distribution along the chain and for the geometry of the system as a whole. In contrast when the N atom is incorporated in either the coronene or corannulene terminations, the angle of relative rotation is less than 10 degrees (for comparison, the benchmark structure presents a small torsion of about 10 degrees).

In order to understand the conductivity channel in the linear chains, the spin-polarized DOS as well as the total spin densities were calculated for these 1N-doped systems. These are displayed in Fig. 3(a) for the structure A1N. The results obtained for the spin-polarized DOS indicate that the electronic ground states of all the systems incorporating 1 N atom are doublet states (see Table I). As mentioned before this feature is related to a localized electronic state that appears near the Fermi level, resulting from the fact that the N atom
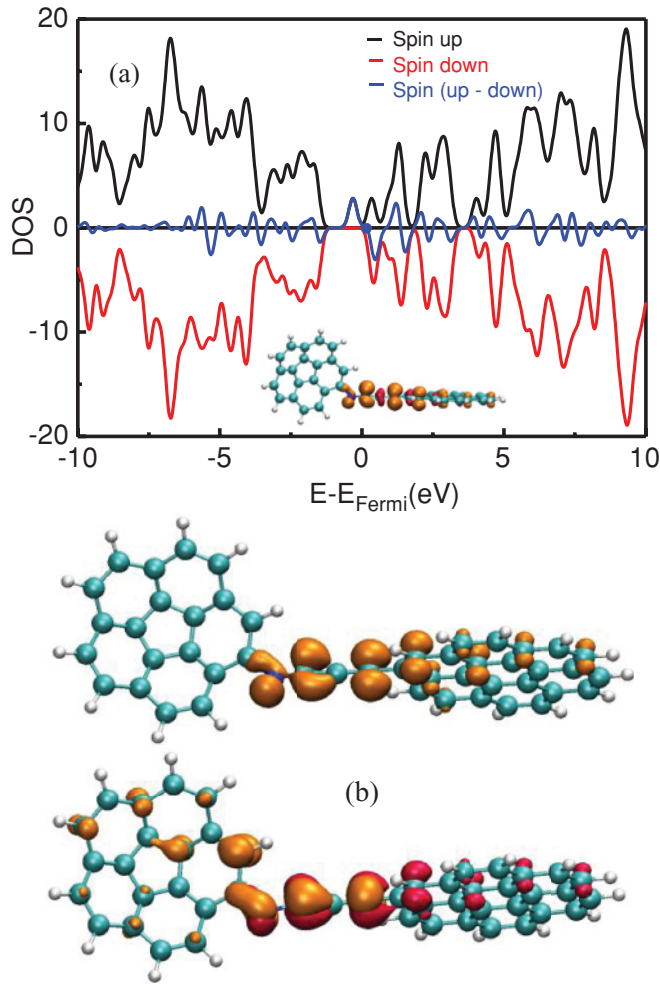
FIG. 3. (Color online) (a) Calculated spin-polarized DOS for A1N. The total spin density is displayed in the inset. (b) Iso-surface of the HOMO (top) and LUMO (bottom) spin densities. Yellow color corresponds to the up-spin density, and red color corresponds to the down-spin density.

TABLE I. Cohesive energy per atom (in eV) and the spin multiplicity of the electronic ground state of the systems A1N–F1N (1N-doped), A2N–J2N (2N-doped), and A3N–F3N (3N-doped).

Structure	$E_{coh/atom}$	State
A0N	8.86	Singlet
A1N	8.80	Doublet
B1N	8.77	Doublet
C1N	8.79	Doublet
D1N	8.80	Doublet
E1N	8.77	Doublet
F1N	8.79	Doublet
A2N	8.73	Triplet
B2N	8.73	Singlet
C2N	8.69	Singlet
D2N	8.73	Triplet
E2N	8.68	Triplet
F2N	8.74	Singlet
G2N	8.70	Singlet
H2N	8.72	Triplet
I2N	8.71	Triplet
J2N	8.71	Triplet
A3N	8.64	Doublet
B3N	8.62	Doublet
C3N	8.63	Doublet
D3N	8.61	Doublet
E3N	8.62	Doublet
F3N	8.67	Doublet

possesses 1 additional valence electron more than the carbon atom. For this reason the calculated HOMO-LUMO gaps are much lower in the systems incorporating 1 N atom (varying between 0.33 and 0.69 eV) than in the pure carbon structure (1.92 eV). These findings for the electronic structure of the systems doped with 1 N agree with results obtained for similar systems by others.[10]

From Fig. 3(a) it is also evident that in A1N, the incorporated N atom induces an electronic state below the Fermi level. Thus, the HOMO-LUMO gap decreases from 1.92 eV in A0N to 0.66 eV in A1N (i.e., a reduction of 66%) and to 0.33 eV in C1N (i.e., a reduction of 83%). It is remarkable that the incorporation of 1 N in the pentagon ring of corannulene leads to the smallest energy gap in the whole 1N-doped series. The total spin density of A1N is shown in the inset of Fig. 3(a). As displayed, the largest spin density is concentrated near to the Fermi level. In Fig. 3(b) we plot the iso-surfaces of the HOMO and LUMO spin densities for A1N. Its charge distribution is significantly influenced by the N atom incorporated in the system (again, in comparison to A0N). This change strictly

corresponds to the change in the bond lengths attributable to the same doping event. Hence, the bonding orbital between atoms 22 and 23 in A1N tends to participate in a π-bond, which slightly decreases the corresponding bond length. A similar behavior is observed for the other 1N-doped structures.

Considering the cohesive energy, the calculated $E_{coh/at}$ for the systems incorporating 1 N atom varies between 8.77 and 8.80 eV, as given in Table I. Structures A1N and D1N are the most stable, while B1N and E1N are the least stable in the 1N-doped series. Thus, an N atom incorporated at sites 21 or 24 leads to the most stable configurations, while an N atom located at the border between the chain and the terminations leads to less stable configurations. In fact carbon chains connected by an N atom (such as in B1N and E1N) to the terminations should possess weaker bonds at these connecting sites than the A0N structure.

Summarizing all the systems with 1 incorporated N atom and analyzing the frontier molecular orbital spin densities, we conclude that the HOMO states are mainly concentrated on the carbon atoms in the chain; e.g., in the bonds 20–21 and 22–23 [see Fig. 3(b)]. A similar behavior is observed even for the total spin density of these systems, as displayed in the inset in Fig. 3(a). However, the π-bond pattern along the chain is completely broken when a nitrogen atom is incorporated in the chain, leading to the previously described large rotational deformation at the terminations. Importantly, as a consequence of the N incorporation, the HOMO-LUMO gap decreases (being the value of this reduction dependent on the location of the N doping), changing significantly the conducting channel in the corannulene–C_4–coronene system.

C. Systems incorporating 2 N atoms

Ten different structures containing 2 N atoms were addressed (A2N to J2N). In comparison to the benchmark structure, 2 significant changes characterize these 2N-doped systems:

(1) Changes in the bond lengths; e.g., the bond length 20–21 in system B2N varies to 1.31 Å as compared to the equivalent bond in A0N (1.42 Å), a change of 0.11 Å. Generally, in the systems incorporating 2 N atoms the bond lengths change more significantly (when compared to the benchmark) than in systems incorporating 1 N atom.

(2) Large rotational deformation of the termination planes. For example, the structures A2N, D2N, E2N, H2N, and J2N exhibit the highest degree of such rotation (of about 90 degrees). The remaining conformations exhibit rotation of approximately 30 degrees, while the reference system presents deformation of only 10 degrees. Following the same pattern as the system incorporating 1 N atom, also the structures containing 2 N atoms in the chain exhibit the largest rotational deformations.

Considering the electronic properties of the 2N-doped systems, we found that their electronic ground state is either singlet or triplet (Table I). In fact we noticed a simple rule defining the multiplicity of the ground state of such systems:

(1) When both N atoms belong to the chain or to the same termination (either the corannulene or the coronene), it is a singlet.

(2) When 1 N atom belongs to the chain and the other one belongs to a termination, the electronic ground state is a triplet.

This means that the incorporation of only 1 of the N atoms in the atomic chain increases the spin multiplicity, which results in an open shell system. In contrast when both N atoms belong to the chain or to the terminations, the electron spins become paired. In Fig. 4 the HOMO densities of 2 representative structures (A2N and C2N) with these multiplicities are displayed. The A2N HOMO presents a large concentration of up-spin density near the Fermi level, while the C2N HOMO presents no liquid spin.

Figure 5(a) displays the spin-polarized DOS for A2N. Similarly to which was observed in Fig. 3, the N atoms at sites 19 and 21 create one localized electronic state below the Fermi level. As a result the HOMO-LUMO gap of A2N decreases
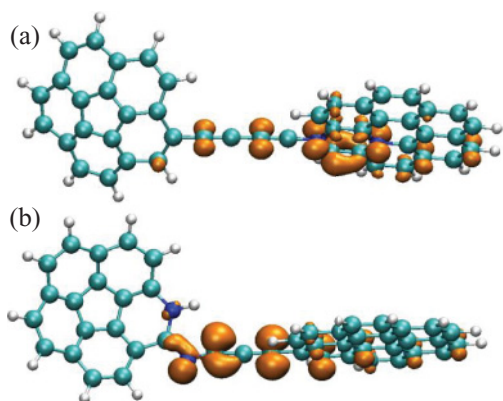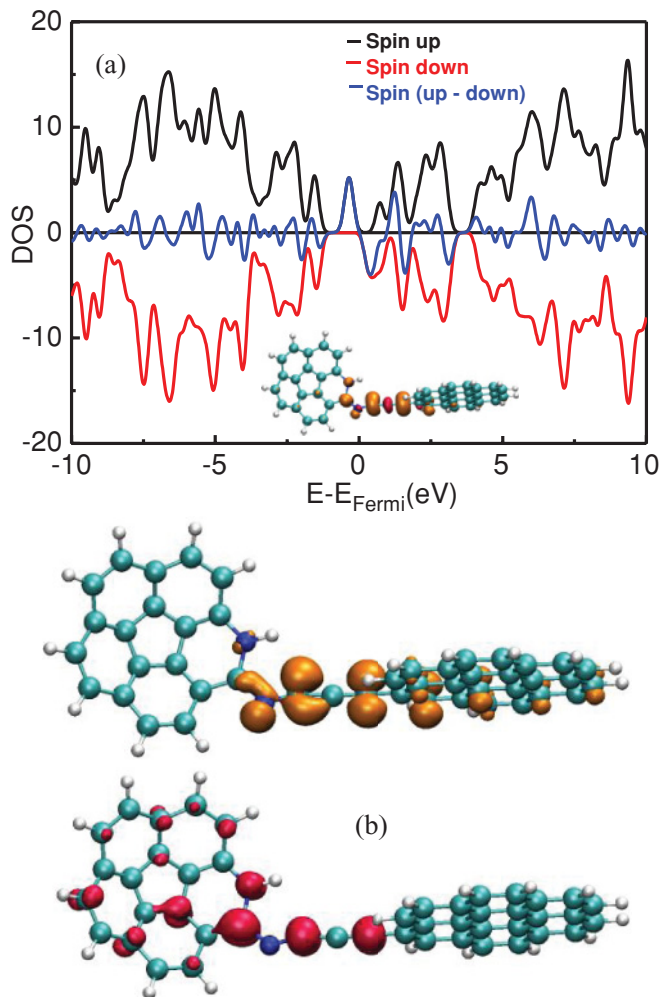

FIG. 5. (Color online) (a) Calculated spin-polarized DOS for A2N. The total spin density is displayed in the inset. (b) Iso-surface of the HOMO (top) and LUMO (bottom) spin densities. Yellow color corresponds to the up-spin density, and red color corresponds to the down-spin density.

FIG. 4. (Color online) Calculated HOMO spin densities for (a) C2N (singlet) and (b) A2N (triplet).

to 0.60 eV in comparison to the A0N structure with energy gap of 1.92 eV. The inset in Fig. 5(a) shows that most of the total spin density of the system is concentrated in the vicinity to its Fermi level. Considering these 2N-doped structures, I2N presents the smallest HOMO-LUMO gap (0.24 eV). Here, a meaningful observation is that the incorporation of another N atom in the pentagon ring at site 1 and another N in the chain at sites 21 or 22 leads to a significant reduction of the HOMO-LUMO gap of these systems.

In Fig. 5(b) the iso-surfaces for the HOMO and LUMO spin densities for A2N are plotted. A considerable amount of the total spin density is concentrated at the atoms in the chain. At atoms 20, 21, 22, and 24, the down-spin density predominates while at atom 23, the down-spin density is more concentrated. The HOMO density is concentrated at the atoms in the chain and also at the bonds 20–21, and 22–23. This charge distribution leads to small changes of the bond lengths 20–21 and 22–23 in comparison to the equivalent bond lengths in the benchmark structure. For example, the bond 20–21
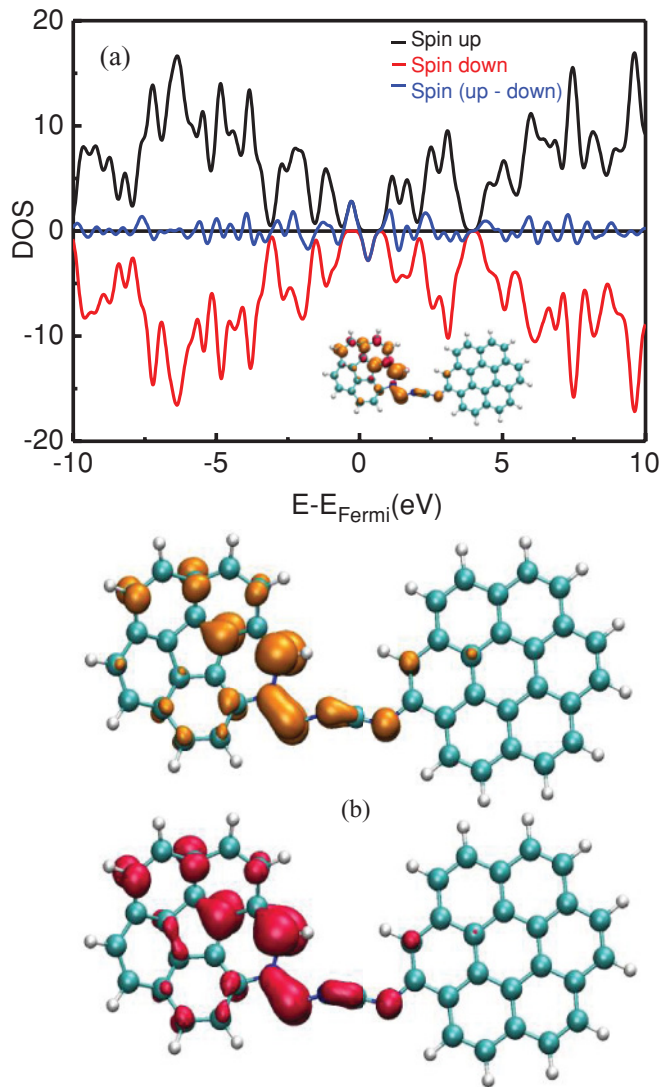
FIG. 6. (Color online) (a) Calculated spin-polarized DOS for F3N. The total spin density is displayed in the inset. (b) Iso-surface of the HOMO (top) and LUMO (bottom) spin densities. Yellow color corresponds to the up-spin density, and red color corresponds to the down-spin density.

1.22 Å, while the corresponding bond length in the benchmark structure is 1.36 Å; i.e., in the structure F3N the contraction (in comparison to the benchmark) in this bond length is 0.14 Å. Another remarkable change in the bond length is noticed in 19–20 of structure A3N, which exhibits the value of 1.50 Å, while in the benchmark structure it is 1.42 Å (an increment of 0.08 Å).

The electronic-ground states of all these system incorporating 3 N atoms are doublet, since they carry an additional valence electron per incorporating site (see Table I). The N doping leads to more energy states below and above the Fermi level, and the HOMO-LUMO gaps decrease in relation to the benchmark structure A0N. For instance in F3N the HOMO-LUMO gap reads 0.58 eV (i.e., a reduction of ~70%), while in C3N this is only 0.22 eV (i.e., a reduction of ~89%), in comparison to the benchmark value of 1.92 eV. All these results present an obvious impact on the chain conductivity of systems incorporating 3 N atoms. Figure 6(a) shows the polarized DOS and the iso-surfaces of the total spin density of F3N. As seen, a large amount of the total spin density is concentrated near to the Fermi level, leading to a concentration of conductive states in this region.

Figure 6(b) displays the HOMO and LUMO spin densities of F3N. A large amount of the total spin density and HOMO density are concentrated in the corannulene molecule and in the atomic chain. Where the chain is connected to the corannulene termination appears spin-rich or spin-poor regions. This result agrees well with works by other groups on similar systems.[34,35] We found that a π-bond is formed between atoms 20 and 21, which decreases the bond length 20–21 to 1.40 Å (1.42 Å in A0N). Bond 22–23 is also a π-bond type which explains its contraction by 0.14 Å, compared to A0N. However, the most important feature of the 3N-doped systems is the disruption of the delocalized π-bond, typical in the benchmark system.

In terms of stability the less energetically stable 3N-doped structure is the system D3N ($E_{coh/at}$ = 8.61 eV), while the most stable is the system F3N ($E_{coh/at}$ = 8.67 eV). Again, these results confirm that N incorporated in the chain leads to a more stable system than N incorporated in the graphenelike terminations. For a better comparison, our calculated values for the 3N-doping series are given in Table I.

E. Overall comparison among the N-doped systems

The electronic ground state of the N-doped carbon nanostructures considered here depends on the number and the location of the N atoms incorporated in the system. As displayed in Table I, structures containing 1 N atom are doublet, those containing 2 N atoms are singlet or triplet, depending on the location of the N incorporation sites, and the structures containing 3 N atoms are always doublet. Table I also lists the calculated $E_{coh/at}$ for all systems addressed. Generally, when the N concentration increases, the cohesive energy per atom decreases as found for similar systems.[36] This result means that the greater the number of N atoms incorporated in a given structure, the less energetically stable it becomes. Thus, the average cohesive energy per atom decreases by about 1% with the inclusion of 1 N atom, 1.7% with the inclusion of 2 N atoms, and 2.6% with the inclusion of 3 N atoms in the benchmark structure A0N.

decreases by 0.07 Å, while the bond 22–23 decreases by 0.05 Å in comparison to A0N.

Among the systems incorporating 2 N atoms, the most energetically stable is F2N ($E_{coh/atom}$ = 8.74 eV) containing the 2 N atoms in the chain. The less energetically stable is E2N with $E_{coh/atom}$ = 8.68 eV and with the 2 N atoms located at the border between the chain and the terminations. N incorporation at sites 21 and 24 implies higher stability than at sites 20 and 25. These results match very well our results for the 1N-doped systems, e.g., A1N ($E_{coh/atom}$ = 8.80 eV) and B1N ($E_{coh/atom}$ = 8.77 eV).

D. Systems incorporating 3 N atoms

We studied six different structures incorporating 3 N atoms (A3N to F3N). Significant structural changes are also observed in comparison with the systems poorer in nitrogen considered above. In the structure F3N the bond length 22–23 becomes
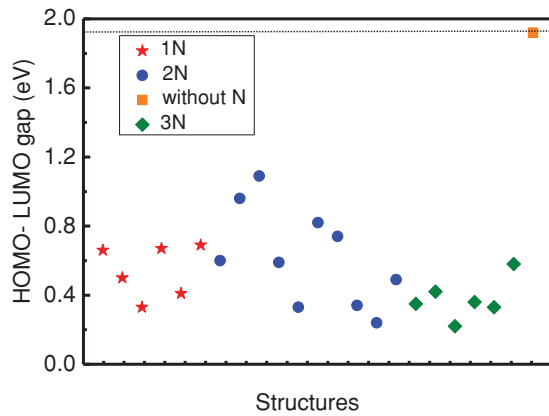
FIG. 7. (Color online) Calculated HOMO-LUMO gap for all the structures studied here. Red stars represent the 1N-doped systems, blue circles the 2N-doped systems, and green lozenges the 3N-doped systems. The gap of the benchmark system is given by an orange square.

Figure 7 illustrates the variation of the HOMO-LUMO gaps for all the 22 systems investigated as a function of the number of incorporated N atoms. As seen in Fig. 7, for systems containing 1 N atom the largest energy gaps correspond to an N atom incorporated in the chain (A1N, D1N, and F1N), and the smallest energy gaps correspond to N sites in the graphenelike terminations (B1N, C1N, and E1N). This reduction in the energy gap is also accompanied by significant structural changes, mainly in the atomic chain. In the cases of 2 N and 3 N atoms incorporated, the distance between the N atoms influences the energy gap value. This can be noticed when we compare directly the gap values for E2N and F2N with those for G2N, H2N, and I2N, and still with those for C3N, E3N, and F3N. The closer the N incorporation sites, the higher the HOMO-LUMO gap. Also, systems which are singlet states exhibit larger energy gaps (Fig. 7) compared to those that are doublet or triplet states.

It is interesting to notice that the effect of N doping in the dispersion of the calculated HOMO-LUMO gaps is higher for systems containing an even number of N atoms. For example, this dispersion in the energy gaps for structures containing 1 N atom is 0.36 eV, for those containing 2 N atoms the dispersion increases to 0.85 eV, and for 3 N atoms it is again 0.36 eV. These findings are worthy for further exploitation of these systems as possible conducting channels in molecular devices.

In fact an N atom incorporated in the low-dimensional carbon system considered in this work (corannulene–C_4–coronene) leads to a reduction of its HOMO-LUMO gap by more than 80%. If the number of incorporated N atoms increases, the HOMO-LUMO gap values generally decrease further or stay low. While the energy gap of the benchmark structure is 1.92 eV, the average energy gap of the systems containing 1 N atom is 0.54 eV, the average energy gap of the systems containing 2 N atoms is 0.62 eV, and the average energy gap of the systems containing 3 N atoms is 0.37 eV. Complementarily, these results indicate that systems containing an odd number of N atoms have smaller HOMO-LUMO gap than systems containing an even number of N atoms.

IV. CONCLUSIONS

We have carried out a detailed spin-polarized DFT study of the structural and electronic properties of carbon-based nanostructures consisting in a small linear chain formed between 2 distinct sp^2 terminations doped with nitrogen in different concentrations. These terminations were chosen as 2 chemically synthesizable (i.e., experimentally viable) molecules, such as coronene and corannulene. We have examined the impact of the substitution of C atoms by N atoms at different concentrations and sites on the HOMO-LUMO gap of the systems. The results suggest that the possible conducting channel of these C-based nanostructures can be controllably tailored by doping the systems with N atoms. Most interesting, the conformation of some doped structures is controlled by the spin states of the system. Also, the rotational deformation of the termination graphenelike pieces depends on the number and the location of the N incorporation sites. The most stable N-doped conformations exhibit relative rotation of the terminations of approximately 90 degrees.

The N-doping effects in these systems correspond to a significant reduction of their HOMO-LUMO gaps and to a considerable change in both their charge distribution and structure. Thus, the energy gap can be tuned in a range between 0.2 and 1.1 eV. In all these cases of N incorporation, the HOMO-LUMO gap decreased more than 60% in comparison to the HOMO-LUMO gap of the pure carbon benchmark structure. For the systems containing 1 N atom, the electronic ground state is doublet. For the systems containing 2 N atoms, the electronic ground state is either a singlet or triplet, depending on the sites of N incorporation. For the systems containing 3 N atoms, the electronic ground state is a doublet.

These results emphasize that N-doped carbon atomic chains connected to graphenelike terminations are promising C-based nano-systems, permitting controllable changes of their electron-spin states and their conductive states near the Fermi level. These features are even more valuable when considered in the context of the feasibility of the experimental fabrication of such nano-systems from GNRs containing nitrogen, by employing, for example, controlled energetic-electron irradiations inside a transmission electron microscope.

*renatobs@ufba.br

†rivelino@ufba.br

‡gekos@ifm.liu.se

[1] Yuchen Ma, A. S. Foster, A. V. Krasheninnikov, and R. M. Nieminen, Phys. Rev. B **72**, 205416 (2005).

[2] J. Berashevich and T. Chakraborty, Phys. Rev. B **80**, 115430 (2009).

[3] S. F. Huang, K. Terakura, T. Ozaki, T. Ikeda, M. Boero, M. Oshima, J. Ozaki, and S. Miyata, Phys. Rev. B **80**, 235410 (2009).

[4] X. Lepró, E. Terrés, Y. Vega-Cantú, F. J. Rodríguez-Macías, H. Muramatsu, Y. A. Kim, T. Hayahsi, M. Endo, M. Torres, and M. Terrones, Chem. Phys. Lett. **463**, 124 (2008).

[5] Y. Shao, G. Yin, and Y. Gao, J. Power Sources **171**, 558 (2007).

[6] S. Stafström, Appl. Phys. Lett. **77**, 3941 (2000).

[7] P. A. Denis, J. Phys. Chem. C **112**, 2791 (2008).

[8] P. A. Denis, J. Mol. Struc. **865**, 8 (2008).

[9] M. N. Groves, A. S. W. Chan, C. Malardier-Jugroo, and M. Jugroot, Chem. Phys. Lett. **481**, 214 (2009).

[10] S. S. Yu, W. T. Zheng, Q. B. Wen, and Q. Jiang, Carbon **46**, 537 (2008).

[11] C. Jin, H. Lan, L. Peng, K. Suenaga, and S. Iijima, Phys. Rev. Lett. **102**, 205501 (2009).

[12] R. Rivelino, R. B. Santos, F. B. Mota, and G. K. Gueorguiev, J. Phys. Chem. C **114**, 16367 (2010).

[13] X. Fan, L. Liu, J. Lin, Z. Shen, and J.-L. Kuo, ACS Nano **3**, 3788 (2009).

[14] I. Hagiri, N. Takahashi, and K. Takeda, J. Phys. Chem. A **108**, 2290 (1994).

[15] M. H. Lai, J. H. Tsai, C. C. Chueh, C. F. Wang, and W. C. Chen, Macromol. Chem. Phys. **211**, 2017 (2010).

[16] T. E. Murphy, D. Y. Chen, E. Cagin, and J. D. Phillips, J. Vac. Sci. Technol. B **23**, 1277 (2005).

[17] W. Jaeger, J. Bohrisch, A. Laschewsky, Progress in Polymer Science **35**, 511 (2010).

[18] A. A. Mohamed, Coord. Chem. Rev. **254**, 1918 (2010).

[19] C. Huang, G. Jiang, and R. Advincula, Macromolecules **41**, 4661 (2008).

[20] J. P. Perdew, J. A. Chevary, S. H. Vosko, K. A. Jackson, M. R. Pederson, D. J. Singh, and C. Fiolhais, Phys. Rev. B **46**, 6671 (1992).

[21] Gaussian 09, Revisions D.01, M. J. Frisch M. J. Frisch, G. W. Trucks, H. B. Schlegel, G. E. Scuseria, M. A. Robb, J. R. Cheeseman, G. Scalmani, V. Barone, B. Mennucci, G. A. Petersson, H. Nakatsuji, M. Caricato, X. Li, H. P. Hratchian, A. F. Izmaylov, J. Bloino, G. Zheng, J. L. Sonnenberg, M. Hada, M. Ehara, K. Toyota, R. Fukuda, J. Hasegawa, M. Ishida, T. Nakajima, Y. Honda, O. Kitao, H. Nakai, T. Vreven, J. A. Montgomery Jr., J. E. Peralta, F. Ogliaro, M. Bearpark, J. J. Heyd, E. Brothers, K. N. Kudin, V. N. Staroverov, R. Kobayashi, J. Normand, K. Raghavachari, A. Rendell, J. C. Burant, S. S. Iyengar, J. Tomasi, M. Cossi, N. Rega, J. M. Millam, M. Klene, J. E. Knox, J. B. Cross, V. Bakken, C. Adamo, J. Jaramillo, R. Gomperts, R. E. Stratmann, O. Yazyev, A. J. Austin, R. Cammi, C. Pomelli, J. W. Ochterski, R. L. Martin, K. Morokuma, V. G. Zakrzewski, G. A. Voth, P. Salvador, J. J. Dannenberg, S. Dapprich, A. D. Daniels, Ö. Farkas, J. B. Foresman, J. V. Ortiz, J. Cioslowski, and D. J. Fox, Gaussian, Inc., Wallingford CT, 2009.

[22] A. D. Becke, J. Chem. Phys. **98**, 5648 (1993).

[23] C. Lee, W. Yang, and R. G. Parr, Phys. Rev. B **37**, 785 (1988).

[24] P. Ordejón, E. Artacho, and J. M. Soler, Phys. Rev. B **53**, R10441 (1996).

[25] J. P. Perdew, K. Burke, and M. Ernzerhof, Phys. Rev. Lett. **77**, 3865 (1996).

[26] N. Troullier and J. L. Martins, Phys. Rev. B **43**, 1993 (1991).

[27] R. Q. Wu, L. Liu, G. W. Peng, and Y. P. Feng, Appl. Phys. Lett. **86**, 122510 (2005).

[28] X. Zhang, Z. Mingwen, Y. Shishen, H. Tao, L. Weifeng, L. Xiaohang, X. Zexiao, W. Zhenhai, L. Xiangdong, and X. Yueyuan, Nanotechnology **19**, 305708 (2008).

[29] M. Nolan and G. W. Watson, Surface Science **586**, 25 (2005).

[30] M. Nolan, S. C. Parker, and, G. W. Watson, Surface Science **595**, 223 (2005).

[31] G. K. Gueorguiev, J. Neidhardt, S. Stafström, and L. Hultman, Chem. Phys. Lett. **401**, 288 (2005).

[32] S. Denifl, B. Sonnweber, J. Mack, L. T. Scott, P. Scheier, K. Becker, and T. D. Märk, Int. J. Mass. Spectrom. **249–250**, 353 (2006).

[33] T. Kato and T. Yamabe, J. Chem. Phys. **117**, 2324 (2002).

[34] K. Fukui, Y. Morita, S. Nishida, T. Kobayashi, K. Sato, D. Shiomi, T. Takui, and K. Nakasuji, Polyhedron **24**, 2326 (2005).

[35] Y. Morita, A. Ueda, S. Nishida, K. Fukui, T. Ise, D. Shiomi, K. Sato, T. Takui, and K. Nakasuji, Angew. Chem. **47**, 2035 (2008).

[36] G. K. Gueorguiev, J. Neidhardt, S. Stafström, and L. Hultman, Chem. Phys. Lett. **410**, 228 (2005).